




Echo Time-Dependent Observed Lung T_1 in Patients With Chronic Obstructive Pulmonary Disease in Correlation With Quantitative Imaging and Clinical Indices

Simon M. F. Triphan, PhD,^{1,2,3*}  Oliver Weinheimer, PhD,^{1,2,3} Marcel Gutberlet, PhD,^{4,5} 
 Claus P. Heußel, MD,^{1,2,3} Jens Vogel-Claussen, MD,^{4,5}  Felix Herth, MD,^{3,6}
 Claus F. Vogelmeier, MD,⁷ Rudolf A. Jörres, MD,⁸ Hans-Ulrich Kauczor, MD,^{1,2,3}
 Mark O. Wielpütz, MD,^{1,2,3} Jürgen Biederer, MD,^{1,2,3} and Bertram J. Jobst, MD,^{1,2,3}
 for the COSYCONET Study Group

Abstract

Background: There is a clinical need for imaging-derived biomarkers for the management of chronic obstructive pulmonary disease (COPD). Observed pulmonary T_1 ($T_1(TE)$) depends on the echo-time (TE) and reflects regional pulmonary function.

Purpose: To investigate the potential diagnostic value of $T_1(TE)$ for the assessment of lung disease in COPD patients by determining correlations with clinical parameters and quantitative CT.

Study Type: Prospective non-randomized diagnostic study.

Population: Thirty COPD patients (67.7 ± 6.6 years). Data from a previous study (15 healthy volunteers [26.2 ± 3.9 years]) were used as reference.

Field Strength/Sequence: Study participants were examined at 1.5 T using dynamic contrast-enhanced three-dimensional gradient echo keyhole perfusion sequence and a multi-echo inversion recovery two-dimensional UTE (ultra-short TE) sequence for $T_1(TE)$ mapping at $TE_{1-5} = 70 \mu\text{sec}$, $500 \mu\text{sec}$, $1200 \mu\text{sec}$, $1650 \mu\text{sec}$, and $2300 \mu\text{sec}$.

Assessment: Perfusion images were scored by three radiologists. $T_1(TE)$ was automatically quantified. Computed tomography (CT) images were quantified in software (qCT). Clinical parameters including pulmonary function testing were also acquired.

Statistical Tests: Spearman rank correlation coefficients (ρ) were calculated between $T_1(TE)$ and perfusion scores, clinical parameters and qCT. A P -value < 0.05 was considered statistically significant.

Results: Median values were $T_1(TE_{1-5}) = 644 \pm 78$ msec, 835 ± 92 msec, 835 ± 87 msec, 831 ± 131 msec, 893 ± 220 msec, all significantly shorter than previously reported in healthy subjects. A significant increase of T_1 was observed from TE_1 to TE_2 , with no changes from TE_2 to TE_3 ($P = 0.48$), TE_3 to TE_4 ($P = 0.94$) or TE_4 to TE_5 ($P = 0.02$) which demonstrates an increase at shorter TEs than in healthy subjects. Moderate to strong Spearman's correlations between T_1 and parameters including the predicted diffusing capacity for carbon monoxide (DLCO, $\rho < 0.70$), mean lung density (MLD, $\rho < 0.72$) and the perfusion score ($\rho > -0.69$) were found. Overall, correlations were strongest at TE_2 , weaker at TE_1 and rarely significant at TE_4 - TE_5 .

View this article online at wileyonlinelibrary.com. DOI: 10.1002/jmri.27746

Received Mar 2, 2021, Accepted for publication May 12, 2021.

*Address reprint requests to: S.M.F.T., Im Neuenheimer Feld 130.3, 69120 Heidelberg, Germany. E-mail: simon.triphan@uni-heidelberg.de

From the ¹Department of Diagnostic and Interventional Radiology, University of Heidelberg, Heidelberg, Germany; ²Translational Lung Research Center Heidelberg, Member of the German Lung Research Center, Heidelberg, Germany; ³Department of Diagnostic and Interventional Radiology with Nuclear Medicine, Thoraxklinik at University of Heidelberg, Heidelberg, Germany; ⁴Institute for Diagnostic and Interventional Radiology, Hannover Medical School, Hannover, Germany; ⁵Biomedical Research in Endstage and Obstructive Lung Disease Hannover, Member of the German Center for Lung Research, Hannover, Germany; ⁶Department of Pneumology and Critical Care Medicine, Thoraxklinik at University of Heidelberg, Heidelberg, Germany; ⁷Department of Medicine, Pulmonary and Critical Care Medicine, University Medical Center Giessen and Marburg, Member of the German Center for Lung Research, Marburg, Germany; and ⁸Institute and Outpatient Clinic for Occupational, Social and Environmental Medicine, Ludwig-Maximilians-Universität München, Munich, Germany

Additional supporting information may be found in the online version of this article

This is an open access article under the terms of the Creative Commons Attribution-NonCommercial License, which permits use, distribution and reproduction in any medium, provided the original work is properly cited and is not used for commercial purposes.

Data Conclusion: In COPD patients, the increase of T_1 (TE) with TE occurred at shorter TEs than previously found in healthy subjects. Together with the lack of correlation between T_1 and clinical parameters of disease at longer TEs, this suggests that T_1 (TE) quantification in COPD patients requires shorter TEs. The TE-dependence of correlations implies that T_1 (TE) mapping might be developed further to provide diagnostic information beyond T_1 at a single TE.

Level of Evidence: 2

Technical Efficacy: Stage 1

J. MAGN. RESON. IMAGING 2021;54:1562–1571.

The clinical assessment of chronic obstructive pulmonary disease (COPD) is traditionally based on clinical history, physical disability, and pulmonary function testing (PFT).¹ X-ray imaging has primarily been used to rule out differential diagnosis, for example, heart failure, infectious complications (pneumonia, bronchopneumonia), and malignancy, but has only limited value for the further classification of COPD.² Increasingly, computed tomography (CT) is used for the regional assessment of the extent and distribution of structural and functional lung alterations, such as emphysema, gas trapping, and airway remodeling.^{3–5} Regarding the heterogeneity of disease manifestation with differentiated options for treatment in patients with different phenotypes of the disease, quantitative imaging-based biomarkers appear to play an increasingly important role for the assessment and monitoring of the disease beyond visual reading and descriptive radiologic reporting.⁶ MRI can provide both regional morphologic and functional assessment of the lungs without radiation exposure.^{7–9} In current practice, dynamic contrast-enhanced (DCE) perfusion imaging is considered the most robust MR technology for assessing obstructive airway disease, reflecting the effect of hypoxic pulmonary vasoconstriction as a surrogate for lung ventilation.^{10–12} In COPD it has been shown to correlate with the degree of emphysematous destruction as quantified with CT.¹³ However, DCE MRI visualizes lung pathology only indirectly and may fail to differentiate between perfusion deficits due to airway obstruction or emphysematous tissue loss.⁷ Furthermore, due to potential adverse events and the possibility of cerebral gadolinium deposition, a method without the need of intravenous contrast material is desirable. T_1 relaxation time maps may serve as an interesting alternative for this purpose. T_1 is a physical parameter that directly correlates with composition and state of lung tissue, including the blood volume fraction.^{14,15} Shorter T_1 values have been observed in the lungs of patients with COPD compared to healthy volunteers.^{15–18} This has led to further developments in T_1 mapping methods, including the inversion recovery radial multi-echo two-dimensional (2D) UTE (ultra-short TE) sequence used in this work.¹⁹ In a small sample of COPD patients, it has been shown that visual abnormalities on T_1 maps correlated well with perfusion deficits in DCE MRI.¹⁵ The study concluded that T_1 reflects the regional pulmonary blood pool and may contribute to the further differentiation of perfusion deficits

demonstrated with DCE MRI. A further study revealed that the observed T_1 in the lungs depends on the echo time it is measured at.²⁰ This is assumed to be due to the presence of essentially two separate compartments of protons in each voxel: firstly, intravascular protons in blood vessels, which exhibit a long T_1 and a very short T_2^* , due to the field inhomogeneities caused by lung structure, and secondly, extravascular protons in the tissue outside the blood vessels, such as alveolar walls, which have a shorter T_1 and an even shorter T_2^* . Accordingly, when measuring T_1 at ultra-short TE, both compartments contribute to the observed T_1 by their volume fraction, but as TE increases, T_2^* weighting results in a signal loss of the extravascular components and a relative predominance of the signal from the intravascular compartment, that is, blood. Being physical parameters, T_1 and T_1 (TE) might provide objective quantitative biomarkers for the local characteristics of pulmonary disease independent of scanner type or observer.²¹ As such, it may have potential to provide an outcome measure for patient stratification and therapy monitoring in clinical trials, without the need for ionizing radiation and intravenous contrast materials.

Thus the aim of this study was to examine the TE-dependence of the correlations between T_1 (TE) and quantitative CT (qCT), DCE MRI and clinical indices in patients with COPD.

Materials and Methods

Patient Characteristics

A total of 30 participants of the German multicenter COPD cohort study COSYCONET (“COPD and SYstemic consequences-COMorbidities NETWORK”, ClinicalTrials.gov Identifier: NCT01245933) were included²² by selecting those patients assigned to a specific study center. The overarching COSYCONET study as well as the part of the imaging-based sub-study (“Image-based structural and functional phenotyping of the COSYCONET cohort using MRI and CT [MR-COPD]”, ClinicalTrials.gov Identifier: NCT02629432) described here were approved by the responsible ethics committees of the coordinating centers (Institutional Review Board of the Medical Faculty of the University of University of Marburg [200/09] and of the University of Heidelberg [S-656/2012], Germany). The participants of the present sub-study gave written informed consent to undergo extensive clinical assessment including lung function testing, noncontrast CT, and morpho-functional MRI. The patient characteristics are summarized in Table 1.

TABLE 1. Patient Characteristics

| | |
|---------------------------|---------------------------|
| Sex distribution | 15 female, 15 male |
| Total no. of patients | 30 |
| Age (years) | 67.7 ± 6.6 (51.0–79.0) |
| Weight (kg) | 74.9 ± 14.7 (49.0–115.0) |
| Height (cm) | 169.2 ± 7.0 (154.0–181.0) |
| BMI (kg ² /cm) | 26.6 ± 4.7 (19.7–39.1) |
| GOLD stage | 1.9 ± 1.3 (0–4) |
| FEV1 predicted% | 58% ± 19% (27%–110%) |

Values are given as mean ± standard deviation with the range in brackets.

Clinical Assessment and Pulmonary Function Testing

Body plethysmography was conducted with the subject in a seated position (MasterScreen Body, E. Jaeger, Hoechberg, Germany) according to the guidelines of the European Respiratory Society and the standards of the American Thoracic Society (ATS), and the European Coal and Steel Community (ECSC) predicted values served as the standard of reference.^{23,24} PFT data collected included the predicted Forced Expiratory Volume in 1 second (FEV1pred%), forced vital capacity (FVC), the Tiffeneau index (FEV1/FVC), and diffusing capacity factor for carbon monoxide (DLCO pred%). Global initiative for chronic Obstructive Lung Disease stage (GOLD) and the smoking history (number of pack-years) were also noted. A full list of the examined parameters is given in Table S1 in the Supplemental Material.

Quantitative Chest Computed Tomography

Paired non-enhanced low-dose chest CT was acquired using a 64-detector row scanner (Somatom Definition AS64, Siemens Healthineers, Erlangen, Germany) in a standardized fashion in inspiratory and end-expiratory breath-hold with slice collimation 0.6 mm, pitch 0.75, tube voltage 120 kVp, tube current time product 35 mAs, and a total effective dose <3.5 mSv. Axial volumetric image reconstructions were performed using a smooth B30f convolution kernel at a slice thickness of 1.0 mm and a reconstruction interval of 0.5 mm. Dose modulation and iterative reconstruction were not applied. Inspiratory and expiratory CT images were analyzed automatically using YACTA (yet another CT analyzer).^{25–28} The qCT parameters mean lung density (MLD), emphysema index (EI %), lung volume (LV), and vessel volume (VV) were determined on the inspiratory CTs. MLD was the mean attenuation of all segmented lung voxels in Hounsfield units (HU) and EI% referred to the fraction of voxels in the lung where that attenuation was below –950 HU.²⁹ LV was the volume of the entire lung as segmented by YACTA, while VV was the volume of only the segmented intrapulmonary blood vessels. Furthermore, parametric response mapping (PRM)³⁰ was performed, which allowed for the linkage of inspiratory and expiratory CT after deformable CT volume

registration. Three PRM measures were derived as previously described: healthy tissue (PRM^{Normal}), functional small airways disease (PRM^{fSAD}), and emphysema (PRM^{Emph}). YACTA also provided multiple measures of airways disease, of which the wall percentage, that is, the fraction of the airway cross section occupied by the walls was considered here. This value was averaged over the 5th to 8th generation of the segmented airways.

Chest Magnetic Resonance Imaging

Morpho-functional MRI was performed with a standardized protocol tailored to the demands of the COPD study employing commercially available T₁-weighted sequences before and after intravenous gadolinium-based contrast administration, T₂-weighted sequences, and first-pass DCE perfusion imaging using a 1.5 T MR scanner (Magnetom Aera, Siemens Healthineers, Erlangen, Germany).^{9,11,12,31} DCE perfusion imaging at a time resolution of 1.7 seconds was obtained using 20 acquisitions of a three-dimensional (3D) gradient echo keyhole sequence with echo sharing (Time-resolved angiography With Stochastic Trajectories [TWIST]; Siemens Erlangen) and intravenous contrast injection of 2 mL gadobutrol 1.0 mmol/mL (Gadovist, Bayer, Leverkusen, Germany) using a power injector at a rate of 4 mL/second, followed by a 30 mL 0.9% NaCl chaser. Perfusion images were acquired in between 40 and 56 5 mm thick slices with 208 × 256 matrix size over 365.63 × 450 mm² field of view. For this, TE = 0.76 msec and a flip angle of 20° were used.

For T₁(TE) mapping, before contrast injection an inversion recovery multi-echo 2D ultra-short TE sequence was employed with five echo times TE_{1–5} = 70 μsec, 500 μsec, 1200 μsec, 1650 μsec, and 2300 μsec as previously described (19,20), with TE₁ considered to be ultra-short. In 27 of 30 patients, two coronal 15 mm slices at a 128 × 128 matrix in a 50 × 50 cm² field of view were acquired, while in the remaining patients, only one slice was acquired. The total acquisitions times were 8 min (2 slices) and 4 min (1 slice). The acquisition was based on golden angle-distributed radial spokes,³² which were reconstructed using a non-uniform Fourier transform implemented in MATLAB (Mathworks, Natick, USA)³³. A total of 6000 spokes were acquired during each measurement and then assigned to images through a sliding window 120 spokes wide and a step-width of 60 spokes. This resulted in 99 images per measurement and with TR = 5 msec, a time resolution of 32 msec over the inversion recovery. For the excitation, half-sine pulses at a flip angle of 6° were used. T₁ maps were calculated from these images at each TE.³⁴

Each measurement was acquired during free breathing and images were reconstructed from 50% of data assigned to expiration, as described previously, using the reconstruction parameters given by Triphan et al.¹⁹ Previously published data from 15 adult healthy volunteers (age range 23–33 years) scanned with an implementation of the same sequence acquired on a different 1.5 T scanner served as a standard of reference.²⁰

MR Image Assessment

MRI, including DCE perfusion MRI, was assessed independently by two readers (HM and CM, 5 years and 4 years of experience, respectively) using the chest MRI score as described previously,^{11,16,31,35,36} with conflicts between the readers being resolved by a third reader

(JB, 22 years of experience): For each lobe including the lingula, the extent of perfusion defects was rated as 0 (no notable defects), 1 ($\leq 50\%$ defect) or 2 ($> 50\%$ defect) and then summed for an overall perfusion score (maximum overall score = 12). Finally, the readers classified each patient into emphysema-type or airways-type COPD based on their overall impression of the visual read.

For $T_1(TE)$ quantification, lung segmentation masks were calculated automatically (for details, see the Supplemental Material) and used to determine median T_1 values at TE_{1-5} and the median absolute differences (MAD) from that average. In patients where two slices were acquired, median values of the included volume were calculated. As a measure of the TE-dependence of T_1 , the mean curvature κ of $T_1(TE)$ was calculated from the first and second numerical derivative for all measurements.¹⁴

Defective lung areas were detected by comparing local $T_1(TE)$ to the overall median value found at the same TE. Voxels where $T_1(TE)$ was lower than the median minus half the standard deviation of T_1 at TE_1 (39 msec) were categorized as defects. Further, defect% was used to refer to the fraction of voxels relative to the entire segmented area that were considered defects.

Statistical Analysis

Data analysis was implemented in Python using SciPy.³⁷ Paired Wilcoxon signed-rank tests were used to determine the significance of the differences in T_1 between echo times. The Bonferroni-Holm method was applied to compensate for the comparison at multiple echo times.

Correlations between T_1 at each TE with clinical metrics were examined by calculating Spearman's ρ . Lung $T_1(TE)$ values published previously for 15 healthy adult volunteers were used as a reference.²⁰ Three levels of statistical significance were considered: A P -value < 0.05 was considered significant.

Results

TE-Dependence of T_1 and Comparison to Healthy Volunteers

The median values of T_1 were $T_1(TE_{1-5}) = 644 \pm 78$ msec, 835 ± 92 msec, 835 ± 87 msec, 831 ± 131 msec, and 893 ± 220 msec. These were all significantly shorter than the previously published median T_1 times at every TE in healthy volunteers previously published.²⁰ T_1 significantly increased from the first echo at $TE_1 = 70$ μ sec to all following echoes ($P < 0.05$), but did not differ significantly from TE_2 to TE_3 ($P = 0.48$), TE_3 to TE_4 ($P = 0.94$), or TE_4 to TE_5 ($P = 0.02$) (Fig. 1a–c). Compared to the previously reported healthy volunteers, observed T_1 increased with TE much more sharply at shorter TEs in the COPD patients. However, when considering the curvature κ of $T_1(TE)$, the mean in COPD patients ($\kappa = -2.6 \cdot 10^{-5} \pm 2.6 \cdot 10^{-5}$) was not significantly different ($P = 0.51$) from that in healthy volunteers ($\kappa = -2.2 \cdot 10^{-5}$) (Fig. 1d). Upon visual assessment, several patients showed an inhomogeneous distribution of T_1 within the lung.

Overall, signal at the longest TE, that is, TE_4 and TE_5 , was extremely low and thus local T_1 was severely distorted. A

typical example is given in Fig. 2 showing representative $T_1(TE)$ maps with corresponding M_0 (proton density) maps from two COPD patients. Corresponding defect% maps are shown in Fig. 3, along with CT images with the segmented vessels and detected emphysema marked. Additional examples taken from patients with varying severity of disease are included in Fig. S2 in the Supplemental Material.

Correlation Between $T_1(TE)$ and Clinical Indices

NON-IMAGING PARAMETERS. Almost all correlations were strongest at TE_2 (Fig. 4), with few exceptions such as the moderate inverse correlation with the reported number of pack years, which showed minimal dependency on TE. Accordingly, example values of ρ at TE_2 (ρ_2) are given here with the full results in Table 2. Median lung $T_1(TE)$ correlated moderately with FEV1 pred% ($\rho_2 = 0.49$, $P < 0.05$) and with FEV1/FVC ($\rho_2 = 0.51$, $P < 0.05$). Among the global, nonimaging parameters, DLCO pred% showed the strongest correlation ($\rho_2 = 0.70$, $P < 0.05$). In the Supplemental Material, correlations with all available parameters are given in Table S1 in the Supplemental Material as well as plots of $T_1(TE)$ against several parameters in Fig. S1 in the Supplemental Material.

Quantitative CT

Overall, $T_1(TE)$ correlated moderately to strongly with the quantitative CT measures MLD ($\rho_2 = 0.72$, $P < 0.05$), PRM^{Normal} ($\rho_2 = 0.69$, $P < 0.05$), EI% ($\rho_2 = -0.69$, $P < 0.05$), and VV/LV ($\rho_2 = 0.58$, $P < 0.05$). Notably, $T_1(TE)$ showed moderate inverse correlations with LV ($\rho_2 = -0.48$, $P < 0.05$), no significant correlations with absolute VV ($\rho_2 = 0.22$, $P = 0.25$) and the highest correlations with VV normalized to LV ($\rho_2 = -0.58$, $P < 0.05$). Correlations with PRM^{fSAD} ($\rho_2 = -0.58$, $P < 0.05$) and PRM^{Emph} ($\rho_2 = -0.62$, $P < 0.05$) were weaker than with PRM^{Normal} ($\rho_2 = -0.69$, $P < 0.05$). The airway measures including the wall percentage were not found to correlate with $T_1(TE)$ ($P = 0.38$). Finally, these correlations showed a similar dependence on TE as T_1 and were weaker at TE_1 than at longer TEs.

DCE Perfusion Scores

A strong inverse correlation was found between $T_1(TE)$ and the perfusion score ($\rho_2 = -0.69$, $P < 0.05$), which was similar at all TE. Finally, at TE_1 a weak correlation ($\rho_1 = -0.44$, $P = 0.016$) implying short T_1 at UTE coincides with the predominance of emphysema as determined by readers was found. However, this was not significant ($P_{2-5} = 0.065$, 0.065 , 0.12 , 0.18) at longer TEs.

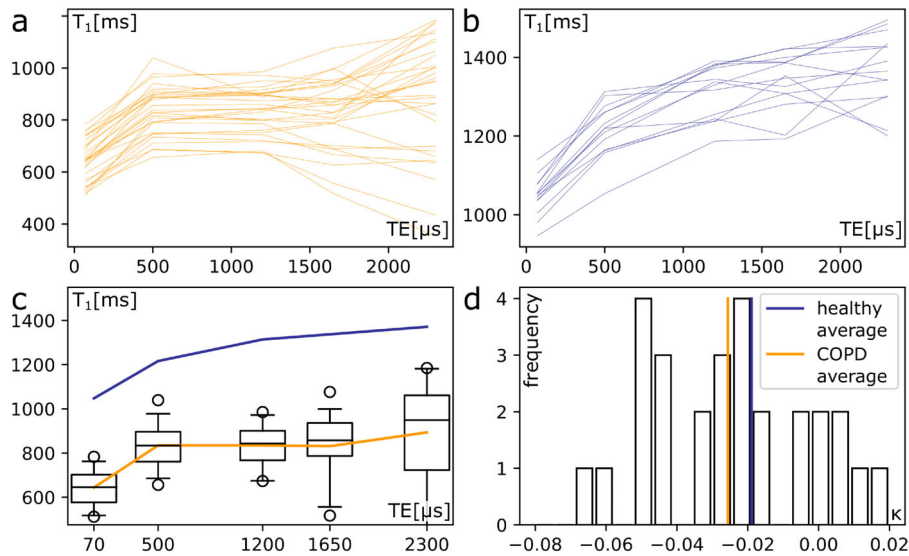


FIGURE 1: Median $T_1(TE)$ relaxation times in patients with chronic obstructive pulmonary disease (COPD) and healthy volunteers. (a,b) Median $T_1(TE)$ from the lungs of all examined COPD patients and healthy volunteers (taken from Triphan et al²⁰). (c) The same data as in (a) and (b), shown as boxplot showing medians and the 1st and 3rd quartiles, whiskers indicating 2nd and 98th percentile for COPD. The orange and blue lines are the overall means from COPD patients and healthy volunteers, respectively. (d) Histogram for the curvature κ of $T_1(TE)$ in COPD patients, with the overall mean shown in grey and the mean for the data from (c) by the dashed line.

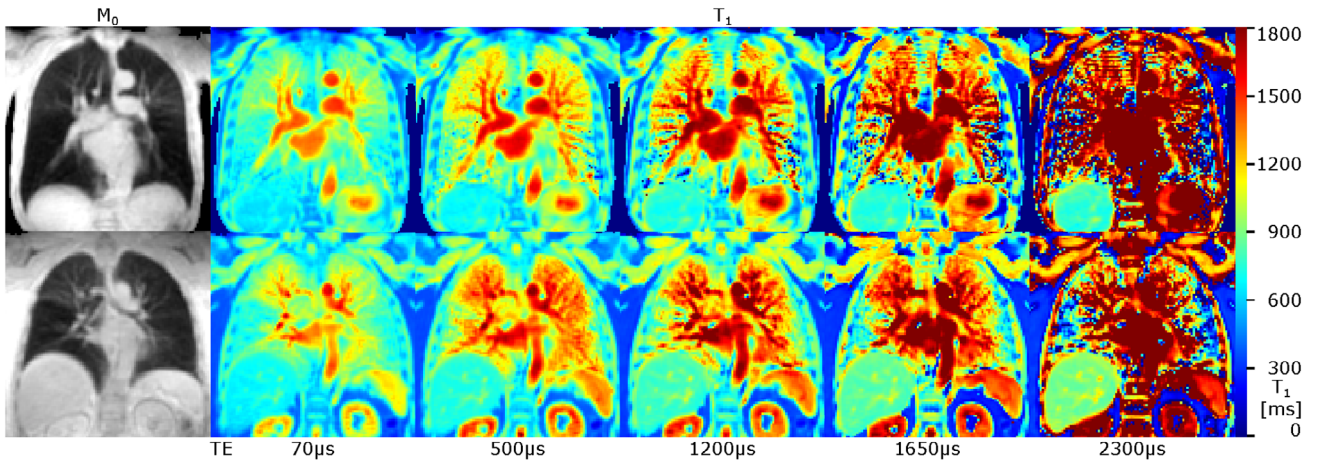


FIGURE 2: Example $T_1(TE)$ maps of two COPD patients at each TE and corresponding M_0 maps at UTE.

Correlation of Defect% With Clinical/Image Indices

An overview of Spearman’s correlations between defect% derived from local T_1 at each TE and several clinical indices is given in Table 3. Correlations with all tested parameters are given in Table S2 in the Supplemental Material.

Overall, defect% correlations were mostly similar to $T_1(TE)$ correlations, except for showing the opposite sign. However, they were generally slightly stronger, especially at UTE, thus reducing but not erasing the TE-dependency of the correlation. Notably, the correlation with VV/LV did not increase. In the correlation with the perfusion score, this led to a higher correlation at TE_1 than at TE_2 .

Discussion

Compared to values previously reported in healthy volunteers,²⁰ lung T_1 values at all TEs in patients with COPD were shorter, as has been previously reported at a single, conventional TE(750 μ sec) for COPD patients alone¹⁵ and in comparison to an age-matched control group.¹⁸ Similar to observations in healthy volunteers, $T_1(TE)$ was found to increase with TE in COPD patients, but this increase occurred only at the shortest echo times, from $TE_1 = 70 \mu$ sec to $TE_2 = 500 \mu$ sec. The TEs employed in this study had been successfully applied in healthy subjects and patients with cystic fibrosis.^{14,20} However, our results

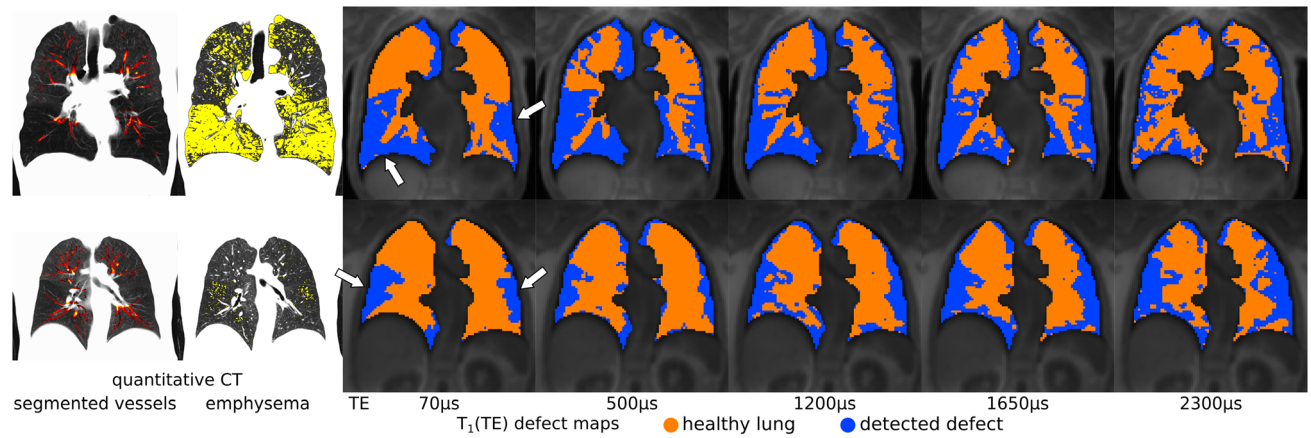


FIGURE 3: Vessels (marked in red) and local emphysema (yellow) detected by quantitative CT and example maps of defects detected using $T_1(TE)$. The $T_1(TE)$ defect maps directly correspond to Fig. 2, and show the same slices. Defects have been highlighted using arrows.

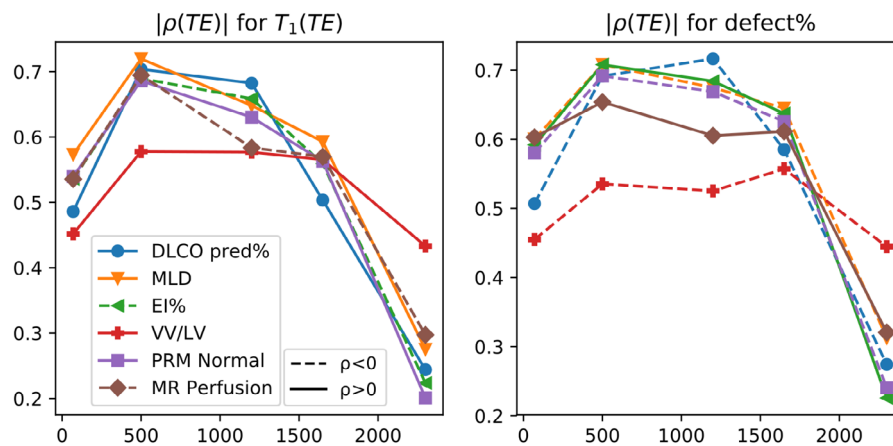


FIGURE 4: Correlations of $T_1(TE)$ and defect% with clinical metrics and quantitative CT, dependent on TE. Inverse correlations are shown as dashed lines and positive correlations are shown using solid lines.

suggest that the ideal set of TEs for sampling the dynamic range which contains relevant T_1 changes should be chosen depending on the presence of suspected pathologies.

The T_1 maps, as well as the disappearance of correlations at TE₄ and TE₅, demonstrated that it was no longer practical to quantify $T_1(TE)$ at TEs that were still feasible in healthy volunteers, most likely due to low signal-to-noise ratio. This might be due to the presence of emphysema causing a reduction of proton density or affecting local T_2^* .

A TE-dependence was visible in most of the investigated correlations with clinical and imaging biomarkers, to varying degrees: correlations of T_1 with almost all parameters were weaker at TE₁ than at TE₂ with the strongest effect in the correlation of T_1 with DLCO pred%. In contrast to this, the weak correlation of T_1 with the predominance of emphysema was only significant at the shortest TE. Together, this implies that $T_1(TE)$ may contain additional diagnostic information beyond T_1 quantified at a single TE.

Inverse correlations of $T_1(TE)$ with perfusion scores and EI% were found, while the correlations with FEV1/FVC,

DLCO pred%, PRM^{Normal}, and VV/LV were positive. This is consistent with correlations between defect% and these indicators having the opposite sign. The moderate correlation between $T_1(TE)$ and LV was also negative, and likely reflects the tendency of lungs to overinflate in more severe disease.

As several of the indicators used for comparison describe a fraction of the lung volume, most notably EI%, the PRM parameters, and the perfusion scores, we used $T_1(TE)$ to calculate defect% as a means of automatic scoring in order to produce a measure that would be more directly comparable. Correlations of defect% with the other indicators notably showed a less pronounced TE-dependency than those of $T_1(TE)$, and were overall slightly stronger. For instance, MLD, which describes a local tissue attribute like $T_1(TE)$, showed overall roughly similar correlations to $T_1(TE)$ and defect%, while VV/LV, an estimate of the total blood volume fraction (including air), correlated better with $T_1(TE)$ than with defect%. It should be noted that the median $T_1(TE)$ that was used here to determine local defects was taken from the patient collective itself and is much lower than

TABLE 2. Spearman's ρ and P Values Between Median T_1 at Each TE and Clinical Parameters

| TE | 70 μ sec | | 500 μ sec | | 1200 μ sec | | 1650 μ sec | | 2300 μ sec | |
|-----------------------|--------------------|--------|-------------------|--------|-------------------|--------|--------------------|--------|--------------------|-------|
| Median T_1 | 644 \pm 78 msec | | 835 \pm 92 msec | | 835 \pm 87 msec | | 831 \pm 131 msec | | 893 \pm 220 msec | |
| MAD T_1 | 240 \pm 147 msec | | 203 \pm 86 msec | | 220 \pm 70 msec | | 282 \pm 85 msec | | 505 \pm 134 msec | |
| | ρ_1 | P_1 | ρ_2 | P_2 | ρ_3 | P_3 | ρ_4 | P_4 | ρ_5 | P_5 |
| FEV1pred% | +0.35 | 0.054 | +0.49 | 0.006 | +0.40 | 0.030 | +0.24 | 0.208 | +0.15 | 0.444 |
| FEV1/FVC | +0.46 | 0.010 | +0.53 | 0.002 | +0.49 | 0.007 | +0.35 | 0.061 | +0.25 | 0.190 |
| Pack years | -0.44 | 0.018 | -0.45 | 0.015 | -0.43 | 0.020 | -0.46 | 0.012 | -0.23 | 0.229 |
| DLCO pred% | +0.49 | 0.006 | +0.70 | <0.001 | +0.68 | <0.001 | +0.50 | 0.005 | +0.24 | 0.194 |
| MLD (Exp) | +0.57 | <0.001 | +0.72 | <0.001 | +0.65 | <0.001 | +0.59 | <0.001 | +0.28 | 0.141 |
| PRM _{Normal} | +0.54 | 0.002 | +0.69 | <0.001 | +0.63 | <0.001 | +0.56 | 0.001 | +0.20 | 0.287 |
| PRM _{ISAD} | -0.45 | 0.012 | -0.58 | <0.001 | -0.49 | 0.006 | -0.52 | 0.003 | -0.22 | 0.241 |
| PRM _{Emph} | -0.44 | 0.015 | -0.62 | <0.001 | -0.59 | <0.001 | -0.51 | 0.004 | -0.14 | 0.471 |
| EI% | -0.54 | 0.002 | -0.69 | <0.001 | -0.66 | <0.001 | -0.56 | 0.001 | -0.22 | 0.235 |
| LV | -0.38 | 0.037 | -0.48 | 0.007 | -0.38 | 0.039 | -0.40 | 0.028 | -0.25 | 0.179 |
| VV | +0.11 | 0.562 | +0.22 | 0.248 | +0.23 | 0.212 | +0.28 | 0.136 | +0.18 | 0.336 |
| VV/LV | +0.45 | 0.012 | +0.58 | <0.001 | +0.58 | <0.001 | +0.57 | 0.001 | +0.43 | 0.017 |
| Wall percent | -0.18 | 0.377 | -0.04 | 0.835 | -0.11 | 0.596 | +0.01 | 0.971 | -0.19 | 0.348 |
| MR Perfusion | -0.54 | 0.002 | -0.69 | <0.001 | -0.58 | <0.001 | -0.57 | 0.001 | -0.30 | 0.111 |
| Predominance | -0.44 | 0.016 | -0.30 | 0.112 | -0.34 | 0.064 | -0.24 | 0.196 | -0.21 | 0.261 |

Shown parameters are: median absolute difference (MAD), predicted forced expiratory volume in 1 second (FEV1pred%), Tiffeneau Index (FEV1/FVC), Global initiative for chronic Obstructive Lung Disease stage (GOLD), number of pack-years, Diffusing capacity of the Lung for Carbon monOxide (DLCO), Mean Lung Density (MLD), Parametric Response Map Normal tissue (PRM_{Normal}), PRM function Small Airways Disease (PRM_{ISAD}), PRM Emphysema (PRM_{Emph}), Emphysema Index (EI%), Lung Volume (LV), Vessel Volume (VV), percentage fraction of airway walls to total cross section (wall percent), MR Perfusion Score and predominance of emphysema phenotype as determined by readers from MRI.

T_1 (TE) in healthy adults at the same TE. A reference value taken from young healthy volunteers would result in almost all lung area in patients with COPD classified as defect. Accordingly, in order to generalize this approach, comparison values derived from a larger, age-matched control group and most likely more than two categories of tissue state would be necessary. In essence, this demonstrates that further parameters can be derived from T_1 (TE) measurements: that this can affect not only the magnitude of the correlations observed but also the degree of TE-dependency suggests that values could be derived that are diagnostically useful beyond the primarily perfusion-dependent T_1 at a single TE.

While it was recently shown¹⁴ that the discussed approach yields a significantly different curvature for T_1 (TE) in children and young adults with cystic fibrosis, no such difference was observed here. Since, as mentioned above,

the TE-dependence of T_1 is observed in this group at very short TEs, the TEs used here cannot sample this dynamic well. Measurements with a higher time-resolution at short TEs may be necessary to yield sufficient precision for the determination of curvature.

Finally, while strong correlations of T_1 (TE) with quantitative CT measures of emphysema and air-trapping as well as MR perfusion scores were found, no correlations were found with the biomarkers applied to larger airways (up to the eighth generation). This is consistent with the assumption that T_1 primarily reflects changes in the composition and perfusion of the lung parenchyma: the strongest correlations were those with qCT markers describing emphysema and vessels, perfusion MRI scores and DLCO. Due to hypoxic vasoconstriction, these are directly linked, while changes in larger airways would only affect very few voxels in T_1 (TE) maps

TABLE 3. Spearman's ρ and P values Between Defect% at Each TE and Clinical Parameters

| TE | 70 μ sec | | 500 μ sec | | 1200 μ sec | | 1650 μ sec | | 2300 μ sec | |
|-----------------------|--------------|------------|---------------|------------|----------------|------------|----------------|------------|----------------|------------|
| Defect% | 36% | $\pm 26\%$ | 37% | $\pm 20\%$ | 37% | $\pm 16\%$ | 40% | $\pm 17\%$ | 45% | $\pm 13\%$ |
| | ρ_1 | P_1 | ρ_2 | P_2 | ρ_3 | P_3 | ρ_4 | P_4 | ρ_5 | P_5 |
| FEV1pred% | -0.40 | 0.028 | -0.41 | 0.023 | -0.46 | 0.011 | -0.31 | 0.101 | -0.17 | 0.376 |
| FEV1/FVC | -0.50 | 0.005 | -0.52 | 0.003 | -0.55 | 0.002 | -0.40 | 0.027 | -0.29 | 0.120 |
| Pack years | +0.42 | 0.022 | +0.44 | 0.016 | +0.40 | 0.030 | +0.44 | 0.017 | +0.27 | 0.152 |
| DLCO pred% | -0.51 | 0.004 | -0.69 | <0.001 | -0.72 | <0.001 | -0.59 | <0.001 | -0.27 | 0.142 |
| MLD (Exp) | -0.60 | <0.001 | -0.71 | <0.001 | -0.67 | <0.001 | -0.64 | <0.001 | -0.31 | 0.093 |
| PRM _{Normal} | -0.58 | <0.001 | -0.69 | <0.001 | -0.67 | <0.001 | -0.63 | <0.001 | -0.24 | 0.200 |
| PRM _{fSAD} | +0.47 | 0.010 | +0.53 | 0.003 | +0.53 | 0.003 | +0.53 | 0.002 | +0.29 | 0.125 |
| PRM _{Emph} | +0.49 | 0.006 | +0.66 | <0.001 | +0.62 | <0.001 | +0.58 | <0.001 | +0.13 | 0.490 |
| EI% | +0.59 | <0.001 | +0.71 | <0.001 | +0.68 | <0.001 | +0.64 | <0.001 | +0.23 | 0.230 |
| LV | +0.46 | 0.010 | +0.50 | 0.004 | +0.39 | 0.034 | +0.42 | 0.020 | +0.23 | 0.217 |
| VV | -0.06 | 0.737 | -0.16 | 0.389 | -0.20 | 0.295 | -0.22 | 0.234 | -0.21 | 0.274 |
| VV/LV | -0.45 | 0.012 | -0.54 | 0.002 | -0.53 | 0.003 | -0.56 | 0.001 | -0.44 | 0.014 |
| Wall percent | +0.13 | 0.518 | -0.04 | 0.854 | +0.09 | 0.672 | +0.04 | 0.830 | +0.14 | 0.471 |
| MR perfusion | +0.60 | <0.001 | +0.65 | <0.001 | +0.61 | <0.001 | +0.61 | <0.001 | +0.32 | 0.084 |
| MR Pred/Em | +0.46 | 0.011 | +0.34 | 0.064 | +0.34 | 0.064 | +0.29 | 0.122 | +0.25 | 0.182 |

Shown parameters are: predicted forced expiratory volume in 1 second (FEV1pred%), Tiffeneau Index (FEV1/FVC), Global initiative for chronic Obstructive Lung Disease stage (GOLD), number of pack-years, diffusing capacity of the lung for carbon monoxide (DLCO), mean lung density (MLD), parametric response map normal tissue (PRM_{Normal}), PRM function small airways disease (PRM_{fSAD}), PRM emphysema (PRM_{Emph}), Emphysema Index (EI%), lung volume (LV), vessel volume (VV), percentage fraction of airway walls to total cross section (wall percent), MR perfusion score and predominance of emphysema phenotype as determined by readers from MRI.

directly. In general, T₁ measurements appear to be a useful biomarker of pulmonary disease reflecting both persistent lung destruction (emphysema) as well as functional impairment due to airway disease, covering a similar spectrum of pathologies compared to DCE perfusion MRI.

Fitting a monoexponential function for a single T₁ at each TE is an approximation. A more accurate representation of both compartments would require fitting two exponentials for T₁ and T₂* as well as the undisturbed (M₀) and equilibrium magnetization (M₀*) in each. Since this model has eight parameters it is not well suited to produce parameter maps due to ambiguity. It might be worthwhile to develop a simplified model which could compensate for this and separate diagnostically useful information, while still describing the underlying physiology.

Limitations

An essential limitation of the T₁(TE) measurements discussed here is that the acquisitions cover only two (and in three

patients, only one) central slices of the lungs. Since the CT and DCE MRI measurements cover the entire lungs, more comprehensive local comparisons could be made using T₁(TE) maps with full lung coverage. Notably, COPD also affects the lungs in an inhomogenous manner and thus itself likely leads to inhomogenous distribution of T₁(TE) as well as the perfusion MR and qCT parameters. An implementation of the method used here employing a single conventional echo time has been demonstrated,³⁸ but a 3D UTE multi-echo implementation will be required to further investigate the diagnostic potential of this approach. This would also make voxelwise correlations between T₁(TE) maps and coregistered quantitative perfusion MR and qCT parameter maps more practical. Furthermore, the much tighter spacing of echoes that would better cover the TE-dependence observed in patients with COPD here would also require adaptations in the sequence design, like an interleaved acquisition of TEs. While this work only features a small number of patients, we would for this reason suggest further

improvements on the measurement technique before applying it in a larger cohort. This should then also include investigating T_1 at multiple TEs in an age-matched control group, noting that T_1 has been shown to depend on age and sex.³⁹ However, this showed that this primarily showed longer T_1 in younger women with the disparity due to sex decreasing with age and no notable age dependency in males.

Clinical Perspective

The evaluation of the presented method is at a very early stage. However, in the context of COPD, methods for the regional analysis of lung function deficits are sought for, with the perspective of more precise diagnosis and follow-up of disease activity and related lung damage for research and individualized therapy. In particular standard, global lung function tests fail to cover regional changes, which defines the need for appropriate functional imaging. Although the underlying mechanisms of the echo-time dependence of observed T_1 due to the influence of tissue compartments are still subject to discussion, the current work supports the hypothesis that this effect is a possible candidate as a diagnostic tool for multi-parametric, compartment-selective imaging of regional lung function. As the detected defects correlate well with results from DCE MRI, T_1 alone might at least serve as a non-contrast enhanced tool for the analysis of lung perfusion, while also providing the possibility of platform- and observer-independent quantitative evaluation. This encourages further research to analyze the diagnostic scope of this approach, with the perspective that TE dynamics might differentiate lung parenchyma even beyond the scope of an alternative to DCE MRI. In a way this potential can be seen analogous to PRM providing a refinement to the emphysema detection (i.e. EI%) in qCT by further differentiating voxels into a permanent component from emphysematous destruction and a variable, reversible component of air trapping from obstructive bronchiolitis.

Conclusion

Compared to healthy volunteers, T_1 (TE) in the lungs of COPD patients was shorter at all TE with an increase of T_1 occurring only at very short TEs. Moderate to strong correlations of T_1 (TE) and defect% derived from T_1 (TE) with clinical indices, especially qCT and perfusion MR scores, were found and showed similar TE-dependences. These correlations disappeared at the longest examined TEs, suggesting that the ideal set of TEs for T_1 (TE) quantification in patients may depend on the presence of pathologies in the parenchyma. Slightly stronger correlations and weaker TE-dependencies of defect% with clinical indicators suggest that it is at least possible to extract additional, potentially useful parameters from T_1 (TE) measurements. Further research on this topic may eventually lead to the development of methods that provide diagnostic information beyond T_1 at single TEs, while also providing quantitative functional information

without the need for contrast agents or evaluation by radiologist readers.

Acknowledgments

This study was supported by the Competence Network on Asthma/COPD (ASCONET) through a grant from the Federal Ministry of Education and Research (Bundesministerium für Bildung und Forschung, BMBF) of the Federal Government of Germany (01GI0884, <http://www.gesundheitsforschung-bmbf.de/en/4214.php>). Contrast medium for MRI was sponsored by Bayer Vital GmbH, Leverkusen, Germany. The funders have no role in study design, data collection and analysis, decision to publish, or preparation of the manuscript. Open Access funding enabled and organized by Projekt DEAL.

REFERENCES

1. Hashimoto N, Wakahara K, Sakamoto K. The importance of appropriate diagnosis in the practical management of chronic obstructive pulmonary disease. *Diagnostics* 2021;11(4):618.
2. Washko GR. Diagnostic imaging in COPD. *Semin Respir Crit Care Med* 2010;31:276-285.
3. Vogelmeier CF, Criner GJ, Martinez FJ, et al. Global strategy for the diagnosis, management, and prevention of chronic obstructive lung disease 2017 report. GOLD executive summary. *Am J Respir Crit Care Med* 2017;195(5):557-582.
4. Coxson HO, Mayo J, Lam S, Santyr G, Parraga G, Sin DD. New and current clinical imaging techniques to study chronic obstructive pulmonary disease. *Am J Respir Crit Care Med* 2009;180(7):588-597.
5. Lynch DA, Austin JHM, Hogg JC, et al. CT-definable subtypes of chronic obstructive pulmonary disease: A statement of the Fleischner society. *Radiology* 2015;277(1):141579-141579.
6. Gesierich W, Darwiche K, Döllinger F, et al. Positionspapier der Deutschen Gesellschaft für Pneumologie und Beatmungsmedizin und der Deutschen Gesellschaft für Thoraxchirurgie in Kooperation mit der Deutschen Röntgengesellschaft: Strukturvoraussetzungen von Zentren für die interventionelle Emphysemtherapie. *Pneumologie* 2020;74(1):17-23.
7. Kirby M, van Beek EJ, Seo JB, et al. Management of COPD: Is there a role for quantitative imaging? *Eur J Radiol* 2017;86:335-342.
8. Biederer J, Beer M, Hirsch W, et al. MRI of the lung (2/3). Why, when, how? *Insights Imaging* 2012;3(4):355-371.
9. Wielputz M, Kauczor HU. MRI of the lung: State of the art. *Diagn Interv Radiol* 2012;18(4):344-353.
10. Hopkins SR, Wielputz MO, Kauczor H-U. Imaging lung perfusion. *J Appl Physiol* 2012;113(2):328-339.
11. Wielputz MO, Puderbach M, Kopp-Schneider A, et al. Magnetic resonance imaging detects changes in structure and perfusion, and response to therapy in early cystic fibrosis lung disease. *Am J Respir Crit Care Med* 2014;189(8):956-965.
12. Wielputz MO, Eichinger M, Biederer J, et al. Imaging of cystic fibrosis lung disease and clinical interpretation. *Fortschr Röntgenstr* 2016;188(09):834-845.
13. Ley-Zaporozhan J, Ley S, Eberhardt R, et al. Assessment of the relationship between lung parenchymal destruction and impaired pulmonary perfusion on a lobar level in patients with emphysema. *Eur J Radiol* 2007;63(1):76-83.
14. Triphan SMF, Stahl M, Jobst BJ, et al. Echo time-dependence of observed lung T1 in patients with cystic fibrosis and correlation with clinical metrics. *J Magn Reson Imaging* 2020;52(6):1645-1654.

15. Jobst BJ, Triphan SMF, Sedlaczek O, et al. Functional lung MRI in chronic obstructive pulmonary disease: Comparison of T1 mapping, oxygen-enhanced T1 mapping and dynamic contrast enhanced perfusion. *PLoS One* 2015;10(3):e0121520.
16. Jobst BJ, Triphan S, Sedlaczek O, et al. Comparative assessment of T1 imaging, oxygen-enhanced MRI and first-pass perfusion MRI in chronic obstructive pulmonary disease at 1.5 Tesla. *Insights Imaging* 2014;5: 340-340.
17. Jakob PM, Wang T, Schultz G, Hebestreit H, Hebestreit A, Hahn D. Assessment of human pulmonary function using oxygen-enhanced T1 imaging in patients with cystic fibrosis. *Magn Reson Med* 2004;51(5): 1009-1016.
18. Alamidi DF, Morgan AR, Hubbard Cristinacce PL, et al. COPD patients have short lung magnetic resonance T1 relaxation time. *COPD: J Chron Obstruct Pulmon Dis* 2016;13(2):153-159.
19. Triphan SMF, Breuer FA, Gensler D, Kauczor H-U, Jakob PM. Oxygen enhanced lung MRI by simultaneous measurement of T1 and T2* during free breathing using ultrashort TE. *J Magn Reson Imaging* 2015;41 (6):1708-1714.
20. Triphan SMF, Jobst BJ, Breuer FA, et al. Echo time dependence of observed T1 in the human lung. *J Magn Reson Imaging* 2015;42(3): 610-616.
21. Stadler A, Jakob PM, Griswold M, Stiebellehner L, Barth M, Bankier AA. T1 mapping of the entire lung parenchyma: Influence of respiratory phase and correlation to lung function test results in patients with diffuse lung disease. *Magn Reson Med* 2008;59:96-101.
22. Karch A, Vogelmeier C, Welte T, et al. The German COPD cohort COS-YCONET: Aims, methods and descriptive analysis of the study population at baseline. *Respir Med* 2016;114:27-37.
23. Quanjer PH, Tammeling GJ, Cotes JE, Pedersen OF, Peslin R, Yernault J-C. Lung volumes and forced ventilatory flows. *Eur Respir J* 1993;6(Suppl. 16):5-40.
24. Miller MR, Hankinson J, Brusasco V, et al. Standardisation of spirometry. *Eur Respir J* 2005;26(2):319-338.
25. Weinheimer O, Achenbach T, Bletz C, Duber C, Kauczor H, Heussel CP. About objective 3-D analysis of airway geometry in computerized tomography. *IEEE Trans Med Imaging* 2008;27(1):64-74.
26. Wielpütz MO, Eichinger M, Weinheimer O, et al. Automatic airway analysis on multidetector computed tomography in cystic fibrosis: Correlation with pulmonary function testing. *J Thorac Imaging* 2013;28(2): 104-113.
27. Konietzke P, Weinheimer O, Wielpütz MO, et al. Quantitative CT detects changes in airway dimensions and air-trapping after bronchial thermoplasty for severe asthma. *Eur J Radiol* 2018;107:33-38.
28. Konietzke P, Weinheimer O, Wielpütz MO, et al. Validation of automated lobe segmentation on paired inspiratory-expiratory chest CT in 8-14 year-old children with cystic fibrosis. *PLoS One* 2018;13(4): e0194557.
29. Hersh CP, Washko GR, Estépar RSJ, et al. Paired inspiratory-expiratory chest CT scans to assess for small airways disease in COPD. *Respir Res* 2013;14(1):42.
30. Galbán CJ, Han MK, Boes JL, et al. Computed tomography-based biomarker provides unique signature for diagnosis of COPD phenotypes and disease progression. *Nat Med* 2012;18(11):1711-1715.
31. Eichinger M, Optazaite D-E, Kopp-Schneider A, et al. Morphologic and functional scoring of cystic fibrosis lung disease using MRI. *Eur J Radiol* 2012;81(6):1321-1329.
32. Winkelmann S, Schaeffter T, Koehler T, Eggers H, Doessel O. An optimal radial profile order based on the golden ratio for time-resolved MRI. *IEEE Trans Med Imaging* 2007;26(1):68-76.
33. Fessler JA, Sutton BP. Nonuniform fast fourier transforms using min-max interpolation. *IEEE Trans Signal Process* 2003;51:560-574.
34. Deichmann R, Haase A. Quantification of T1 values by SNAPSHOT-FLASH NMR imaging. *J Magn Reson Imaging* 1992;96(3):608-612.
35. Stahl M, Wielpütz DMO, Graeber DSY, et al. Comparison of lung clearance index and magnetic resonance imaging for assessment of lung disease in children with cystic fibrosis. *Am J Respir Crit Care Med* 2017;195(3):349-359.
36. Jobst BJ, Wielpütz MO, Triphan SMF, et al. Morpho-functional 1H-MRI of the lung in COPD: Short-term test-retest reliability. *PLoS One* 2015; 10(9):e0137282.
37. Virtanen P, Gommers R, Oliphant TE, et al. SciPy 1.0: fundamental algorithms for scientific computing in Python. *Nature Methods* 2020;17 (3):261-272. <https://doi.org/10.1038/s41592-019-0686-2>.
38. Triphan S, Wielpütz M, Kauczor H-U, Jobst B. 3D T1 mapping in the lungs during free breathing using asymmetrical cylindrical encoding. In: ISMRM Annual Meeting. Paris; 2018.
39. Kindvall SS, Diaz S, Svensson J, Wollmer P, Slusarczyk D, Olsson LE. Influence of age and sex on the longitudinal relaxation time, T1, of the lung in healthy never-smokers. *J Magn Reson Imaging* 2016;43(5): 1250-1257.